Chemical Papers (2022) 76:1031–1043
https://doi.org/10.1007/s11696-021-01923-1

ORIGINAL PAPER

Synthesis of silver nanoparticles by plant extract, incorporated into alginate films and their characterizations

Apparao Gudimalla[1,2,3] · Jiya Jose[2] · Jose Varghese Rajendran[2] · Giridhar Gurram[1] · Sabu Thomas[2]

Received: 29 March 2021 / Accepted: 6 October 2021 / Published online: 15 October 2021

Abstract

It is interesting to synthesize materials by an eco-friendly method for wound healing and other applications. Herein silver nanoparticles (AgNPs) were synthesized by an eco-friendly method using *Justicia adhatoda* leaf extract. The synthesized AgNPs were incorporated with sodium alginate (SA) to make films that can be used for wound healing and many other applications. The prepared AgNPs and the AgNPs incorporated SA films were characterized by TEM, AFM, SEM, optical microscopy, UV–Visible spectrophotometer, FTIR, contact angle, and mechanical analysis. AgNPs exhibited maximum absorbance at 420 nm by UV–Visible spectroscopy, and the TEM images revealed the spherical shape of the AgNPs. Both AgNPs and films showed good antibacterial activity against *Staphylococcus aureus* and *Escherichia coli*. These prepared films can be used for biomedical and nanobiotechnology fields.

Keywords AgNPs · Biosynthesis · Alginate · Antimicrobial activity · Films

Introduction

In recent years, global research and development (R&D) on the field of silver nanoparticles (AgNPs) have found various applications owing to their shape/size-dependent electrical/optical properties and their biological relevance. One of the main reasons for the exponential rise of research potential in AgNPs is the broad range of applications such as in optics, catalysis, quantum dots, solar energy absorption**,** antibacterial & anticancer treatment, biosensing, imaging, and nano-biotechnology (Ali et al. 2016; Iravani 2011; Zain et al. 2014; Pauksch et al. 2014; Sanpui et al. 2011). Nano-biotechnology is emerging as a rapidly growing field as integration between biotechnology and nanotechnology for developing biosynthetic and eco-friendly technology to manufacture new materials at the nanoscale level (Barabadi 2017). Nanomedicines can play a significant role in developing alternative and more effective treatment strategies for treating many diseases (Shi et al. 2017).

Generally, AgNPs can be synthesized through chemical and physical methods such as electrochemical, photochemical, chemical reductions, and heat vaporization (Zhang and Su 2012; Roldán et al. 2014). These conventional methods require several chemicals, and it is quite expensive, toxic, require high energy consumption, and lead to hazardous byproducts (Nabikhan et al. 2010). To overcome these problems, a 'green synthetic protocol' was developed (Franci et al. 2015). Plants offer a good platform for the green synthesis of NPs because they are non-toxic and naturally act as a capping/reducing agent. This method is economically feasible, environmentally friendly, easy to handle, and one-step methodology (Tetgure et al. 2015). Plant leaf and other plant parts like fruit, bark, fruit peels, root, and callus are also used to synthesize Ag, Au, Pt, and metal NPs in several sizes and shapes (Tetgure et al. 2015; Krishnaraj et al. 2010). Nevertheless, the synthesis of metallic NPs has attracted significant interest due to their unique properties. Thereby, the focus has been shifted to the biosynthesis of metallic NPs using plants, microorganisms, algae, etc. (Khatua et al. 2020).

Alginate is a naturally derived polymer and has had a great interest in different areas of nanomedicine for

✉ Apparao Gudimalla
appigspl@yahoo.in; appigspl@gmail.com

[1] Department of Nanotechnology, Acharya Nagarjuna University, Guntur, Andhra Pradesh 522510, India

[2] International Inter University Center for Nanoscience and Nanotechnology, Mahatma Gandhi University, Kottayam, Kerala 686560, India

[3] Jožef Stefan International Postgraduate School, Jamova cesta 39, 1000 Ljubljana, Slovenia

several decades (Ionita et al. 2013; Rani et al. 2013). It has extensive properties such as renewability, biocompatibility, biodegradability (Gudimalla et al. 2020) and can easily modify its surface. Moreover, the similarity of these materials to human tissues supports these materials in wound healing applications (Puppi et al. 2014). It is a natural polymer composed of (1 → 4)—concerted β–D-mannuronic (M) and α–L-guluronic (G) linkages in various covalent blocks. It is a perfect matrix for wound healing materials (Daemi et al. 2017; Ali et al. 2013; Galus and Lenart 2013). Sodium alginate (SA) is a water-soluble polymer (Karakasyan et al. 2015), and it can be easily cross-linked with Zn^{2+}, Ca^{2+}, Ba^{2+}, and Cu^{2+} (Kulkarni et al. 2012). SA films have hydrophilic nature but have low mechanical properties. With the help of cross-linking, the hydrophilic nature can be reduced, and mechanical properties can be improved (Olivas and Barbosa-Cánovas 2008). SA has been coupled with many NPs for various applications. AgNPs incorporated alginate films have been primarily used for biomedical applications due to their good antimicrobial activity, high surface area, thermal stability, unique magnetic, optical, catalytic, and electrical properties (Orsuwan et al. 2016). It is also widely used for cartilage, bone and soft tissue regeneration (Matricardi et al. 2013), controlled-release delivery system (Duceppe and Tabrizian 2010), wound dressing (Han et al. 2010), membrane application (Ma et al. 2014), etc. Nowadays, researchers focus on developing materials with fast wound healing properties (Sikareepaisan et al. 2011).

In the present work, we have developed a novel polymeric nanocomposite film that could be employed as wound dressing, drug delivery system, antimicrobial protection, biological sensor. Herein we 'green' synthesized AgNPs using *Justicia adhatoda* plant leaves and incorporated into SA films for the first time. Many researchers have been reported AgNPs synthesis by using SA as a reducing agent. Still, in the present report, the plant extract is used as a reducing and capping agent, and SA is used as a matrix to cast the nanocomposite films. The surface morphology, surface plasmon resonance of the nanoparticle, morphological, mechanical, water sensitivity tests, wet ability, and antimicrobial activity of the developed nanocomposites were examined and compared with previous works.

Materials and methods

Materials

Adalodakam (*Justicia adhatoda*) leaves were collected from Kottayam, Kerala, India. $AgNO_3$ (99%), $ZnCl_2$ (98%), Sodium Alginate, Glycerol (99%), Nutrient broth, and Agar were purchased from Sigma-Aldrich.

Preparation of plant extract

Adalodakam plant leaves were collected and washed thoroughly three times with tap water and then deionized water to remove the impurities. The leaves were dried in sunlight for one hour and in the oven for 1 h at 90 °C. The leaves were powdered, and 0.5 gm was added to 25 mL of sterile distilled water. Then the mixture was placed in a water bath at 95 °C for two hours and filtered with Whatman No. 1 paper.

Synthesis of silver nanoparticles

The prepared extract was used as a reducing and stabilizing agent for the bio-reduction process (Ahmed et al. 2016). To synthesize the AgNPs, the plant extract (500 µL) was mixed with 1 mM silver nitrate (5 mL) solution, and then the system was kept at 95 °C in a boiling water bath for 5 min (Gudimalla et al. 2020) shown in Fig. 1. The progress of the synthesis was observed by color change, from pale light color to light yellow for confirmation of AgNPs. The color change is due to the reduction of silver ions with the assistance of biomolecules in the plant extract. This might be owing to the surface plasmon resonance (SPR) vibrations.

Preparation of AgNPs loaded films

The solutions were prepared by mixing 1%, 2%, and 4% of SA powder with distilled water with the help of a magnetic

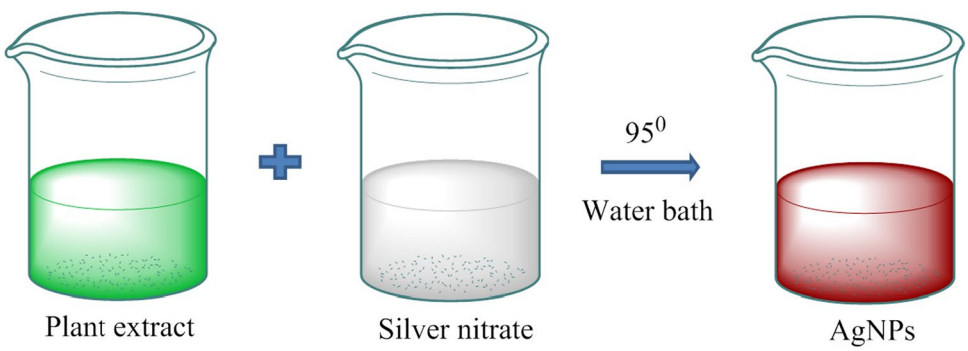

Fig. 1 Synthesis of silver nanoparticles by using *Justicia adhatoda* plant extract

stirrer at 70 °C, for 30 min. After that, the solution was kept outside for 5 min to remove the CO_2. Then 10 ml of SA solution was used to cast the films, then casted film was dried for 24 h at room temperature. Then the films were placed in the oven at 45 °C for 10 min. Then 5% of the $ZnCl_2$ solution was added to the dried films for cross-linking (1 h). To eliminate the traces of the $ZnCl_2$ solution, the films were washed with distilled water. Similarly, AgNPs incorporated films were prepared by mixing an equal amount (1:1) of SA and AgNPs solution and cast, as shown in Fig. 2.

Observation of films preparation

Few drops of glycerol are used as a plasticizer to avoid the premature breaking of the films. SA solution was optimized for the film casting; less polymer solution causes quick breaking, and higher concentration causes thick and slow drying of films due to high water content. The films were dried at room temperature, and the optical images of the prepared composite films are shown in Fig. 3. In the present study, we used 2% of films for characterization and other studies. Hence, it had a smooth surface, medium thickness, and it was not bending or breaking.

Characterization techniques

Microscopy analysis

The TEM analysis was used to study the size, surface morphology, and disparities. TEM observations were performed using the JEM-2100F instrument at the voltage of 200 kV. The FE-SEM analysis was used to study the surface morphology and dispersion of NPs. The AE film was examined by the FE-SEM Model JEOL 7610F. The AFM images of AE film were taken by Alpha 300 RA AFM & RAMAN at a scan rate of 1 Hz, and tapping mode was used to check the morphology of the film.

Spectrometry analysis

The UV–Vis was used to confirm the formation of AgNPs. Bio-reduction of AgNPs and AgNPs loaded (AE) films was characterized by the instrument Cary 5000 UV–Vis-NIR spectrophotometer (scanning range 200–800 nm). Equal amounts of the solution (2.5 mL) were taken, and film sample directly was taken, and the entire sample was analyzed at room temperature.

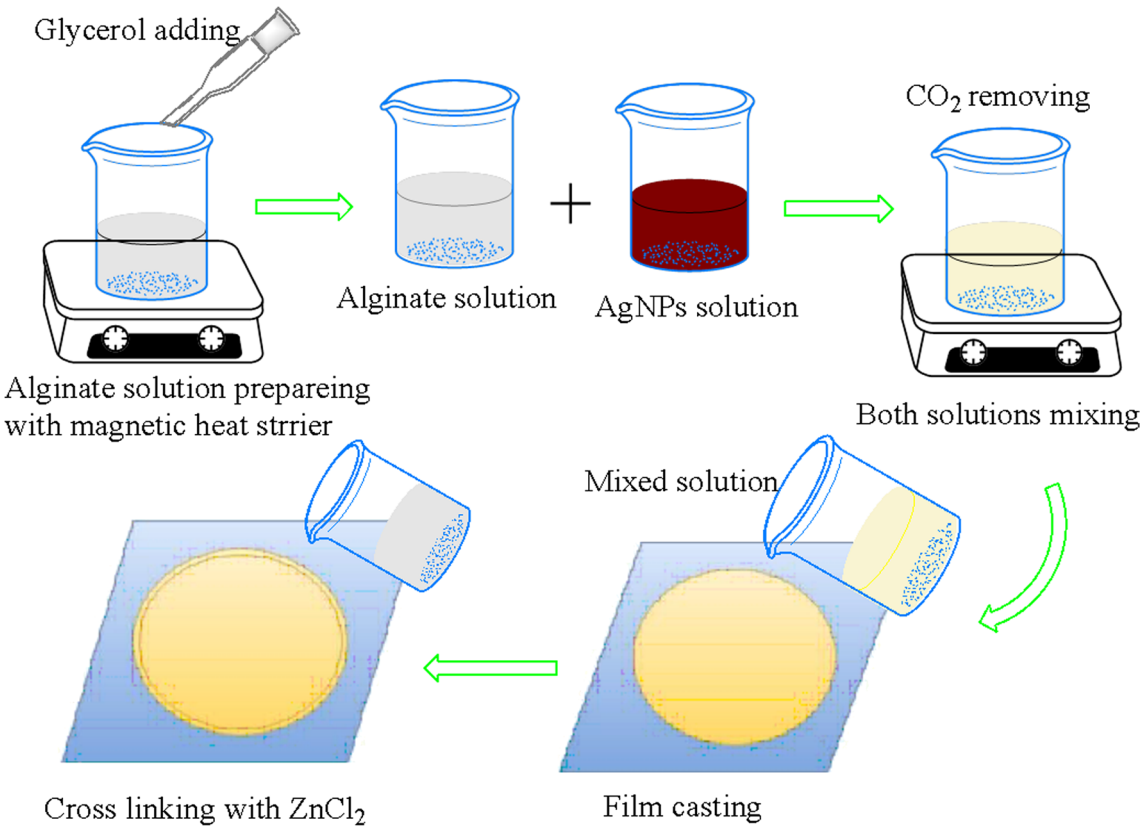

Fig. 2 Silver nanoparticles loaded sodium alginate films preparation (Gudimalla et al. 2020)

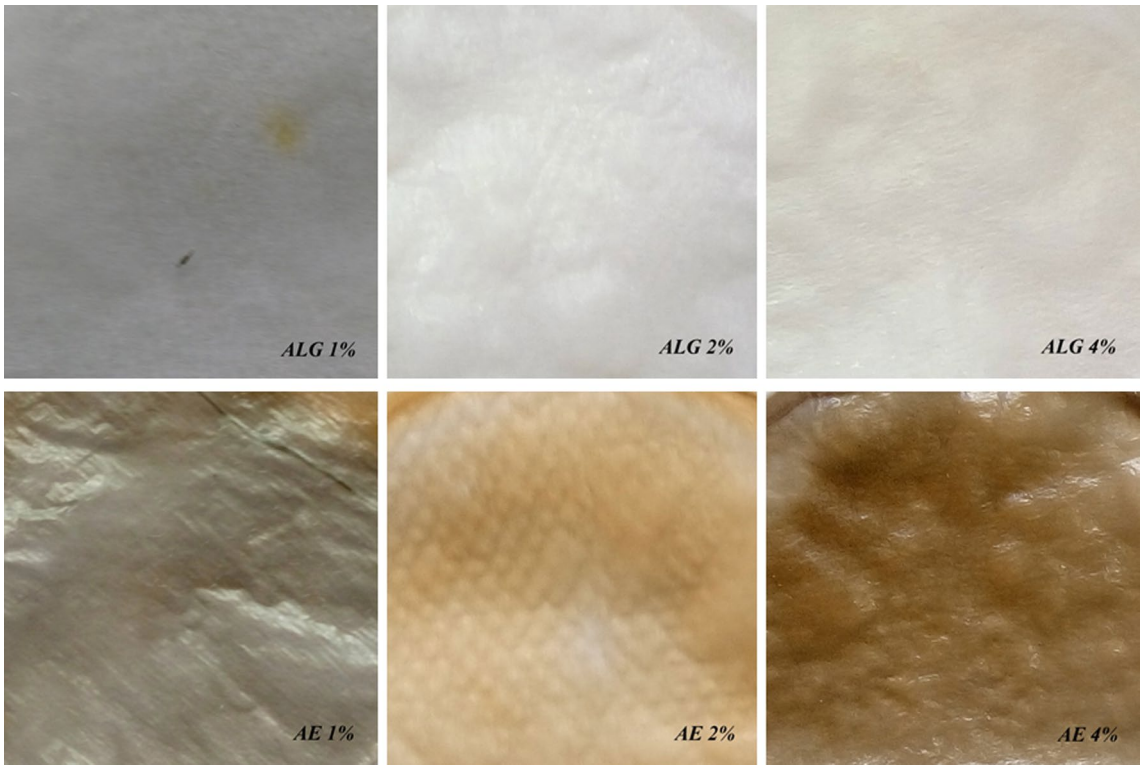

Fig. 3 Prepared film images (ALG-Neat sodium alginate films with different concentrations), (AE-AgNPs incorporated films with different concentrations)

For FTIR measurements, the green synthesized AgNPs solution was taken directly, and similarly, AE films were also analyzed to identify the chemical structure and potential interactions between SA and AgNPs. For each spectrum, the measurements were performed in a range from 4000 to 400 cm^{-1}.

Contact angle measurement

The contact angle measurement was characterized by using SEO Phoenix. The prepared SA and AgNPs incorporated films were cut into 1 × 3 cm rectangular pieces and placed on the stage. The sessile drop method was performed, using deionized water as a reference.

Physical properties of films

Mechanical strength

The tensile properties of the SA film samples (1 × 5 cm) were measured using a Universal testing machine (Tinius Olsen) model H 50 KT, at a crosshead speed of 1 mm/min using a 100 N load cell. The tensile strength, Youngs Modulus and percentage of elongation were measured from the stress–strain graph.

Film thickness Alginate and AgNPs loaded film thickness were measured using a manual Vernier caliper (SNE digital) with a 0.01 mm accuracy. Five consecutive readings were taken at different positions for each sample.

Moisture content To determine the film's moisture content, samples were kept at room temperature and weighed and dried in an oven at 105 °C (24 h.). After this period, the samples were conditioned at room temperature for stabilization of film temperature. Finally, films were weighed and calculated the percentage of film moister content using the following equation.

$$\text{Moister content } (\omega) = \frac{W_1}{W_0} \times 100$$

where W_1 corresponds to the dry weight and W_0—initial weight.

Water soluble: The moisture content weight fraction ω, of the films, was placed in a hot air oven at 105 °C for 24 h. Then the dried films were weighed (M_o) and dipped in distilled water (100 mL) in a beaker (250 mL). Afterward, the beaker was placed on the magnetic stirrer (100 rpm) for 24 h at 25 °C. The final residue was dried in a hot air oven for 24 h at 105 °C,

and then the final weight (M_f) of samples was determined. Solubility was calculated by the following equation.

$$\text{Soluble in water (WS)} = \frac{M_0 - M_f}{M_0} \times 100$$

where M_0 is an initial weight, and M_f is the final weight.

Swelling and absorption First, film samples were dried in a hot air oven to remove the moisture at 105 °C for 24 h. After that, the films' initial mass (W_0) was taken and placed in 10 mL of distilled water at room temperature. The wet samples were taken out, removed the excess water with the help of filter paper, and reweighed (W_1). We need to consider different time intervals for swelling studies, and for absorption studies, only 24 h required. The amount of the water absorbance was calculated by the following equation.

$$\text{Water absorption} = \frac{W_1 - W_0}{W_0} \times 100$$

where W_1 is the final weight, and W_0 is the initial weight.

Antibacterial activity

Biosynthesized AgNPs and AgNPs incorporated (AE) films antimicrobial activity was tested on two types of strains (Gudimalla et al. 2020). One was Gram-negative *Escherichia coli* (*E. coli*), and the second one was Gram-positive: *Staphylococcus aureus* (*S. aureus*). *E. coli* causes infections such as septicemia, enteritis, foodborne illnesses, and urinary tract infections, which are more concerning due to antibiotic resistance. Staphylococcal skin infections are common and cause skin blemishes, pimples, and more painful and concerning issues, such as skin boils, impetigo, abscesses, and cellulitis folliculitis. The antimicrobial activity was investigated by utilizing the nutrient agar well diffusion method for AgNPs and the disk diffusion method for AE film. The culture medium was prepared a day before the experiment. The tested microorganisms were swabbed uniformly on nutrient agar–agar plates using a sterile cotton swab, and then four wells were created in every plate with a 6 mm diameter. The prepared AgNPs were poured in wells of 25 µL, 50 µL, 75 µL and 100 µL concentration of solutions, and AE films were cut into small pieces (3.5 mm diameter) and placed on the swabbed plate surface. Then the plates were incubated for 24 h at 37 °C for the microorganism and bacteria cultures to grow. The diameter of the inhibition zones was measured.

Results and discussion

UV–visible spectrophotometer

UV–visible absorption spectroscopy is an excellent technique to demonstrate the presence of NPs. The biosynthesized AgNPs from plant extract are shown in Fig. 4a and the calibration cover of AgNPs. It was used to study the presence of AgNPs, reduced from silver nitrate with the help of plant extract. Here, the plant extract act as a capping and reducing agent (Ag^+ ion into Ag). AgNP exhibits yellowish-brown due to SPR. A schematic representation of surface plasmon oscillation under the effect of an electromagnetic field and surface plasmon vibrations excitation of AgNPs was reported in Ref. (Barabadi et al. 2019). It is well known that any plant extract mixed with the solution of $AgNO_3$ produces AgNPs, which is indicated by a color change to yellowish-brown. This color deviation is caused by the excitation of a metal nanoparticle of SPR. As the reaction time is prolonged, there will be an increase in the number of particles present in the solution with uniform size

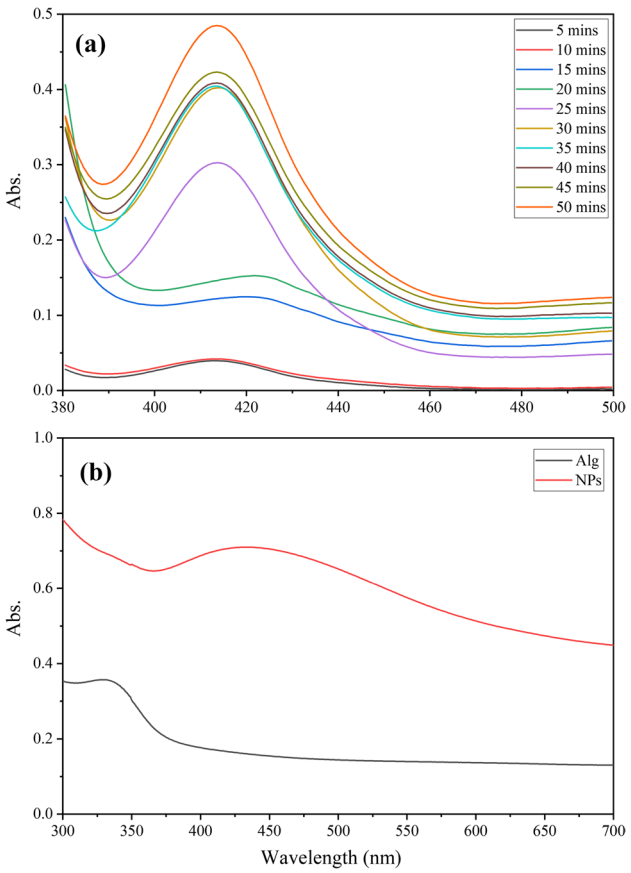

Fig. 4 UV–Vis absorbance **a** spectrum showing the surface plasmon resonance of AgNPs, **b** UV peak of AgNPs loaded alginate film and neat sodium alginate film

distribution (Jemilugba et al. 2019). Many literatures have been reported on the reaction between $AgNO_3$ and plant extract (Ahmed et al. 2016). AgNPs have electron density around them, which gives rise to the SPR absorption band due to the combined vibration of AgNPs in resonance with the light wave (Gudimalla et al. 2020). The AgNPs synthesized using plant extract were analyzed using UV–Vis spectrophotometer by scanning the samples between the range of 200–800 nm, which gave the λ_{max} value between 400 and 430 nm Fig. 4a. The UV spectrum of AgNPs has a sharp absorbance peak at 415 nm. Depending upon size and morphology, Ag NPs absorb in the range of 380–470 nm. The smaller the wavelength of absorption smaller is the size, and vice versa. Absorption at 460 nm means particles is big but still in the nano range, but absorption above 470 nm causes aggregation and precipitation, then it is just silver. So, from our results, we can conclude that the AgNPs are in nano regime.

The absorption spectrum of AgNP loaded film is shown in Fig. 4b. It was observed that the absorption peak around 420 nm is due to the absorption of AgNPs surface plasmon resonance band. The presence of a perfect peak at 420 nm even at a low concentration can be due to SA, which acts as a reducing agent (Azlin-Hasim et al. 2016). This could be confirmed further with the absorption spectra of the control film (neat SA) obtained at around 340 nm. The morphological analysis also could support the AgNPs dispersion on the SA film surface.

Transmission electron microscopy

TEM has been used to classify the surface morphology, shape, and size of the NPs. Typical TEM images of biosynthesized AgNPs from adalodakam plant extract are shown in Fig. 5. As synthesized, AgNPs were drop-coated to a film, and images were taken. Using *image J* software, we calculated the average size as 15 ± 10 nm with a size range of 2–14 nm, and the graph is presented in Fig. 5d. The NPs were homogeneous and spherical. The diffraction pattern shown in Fig. 5c indicates the AgNPs crystalline nature. Also, it shows white dots in the Selected Area Electron Diffraction (SAED), which means the crystalline nature of AgNPs (Arunachalam et al. 2013). NPs were enclosed with other material by pale, slight layer; it is supposed to select

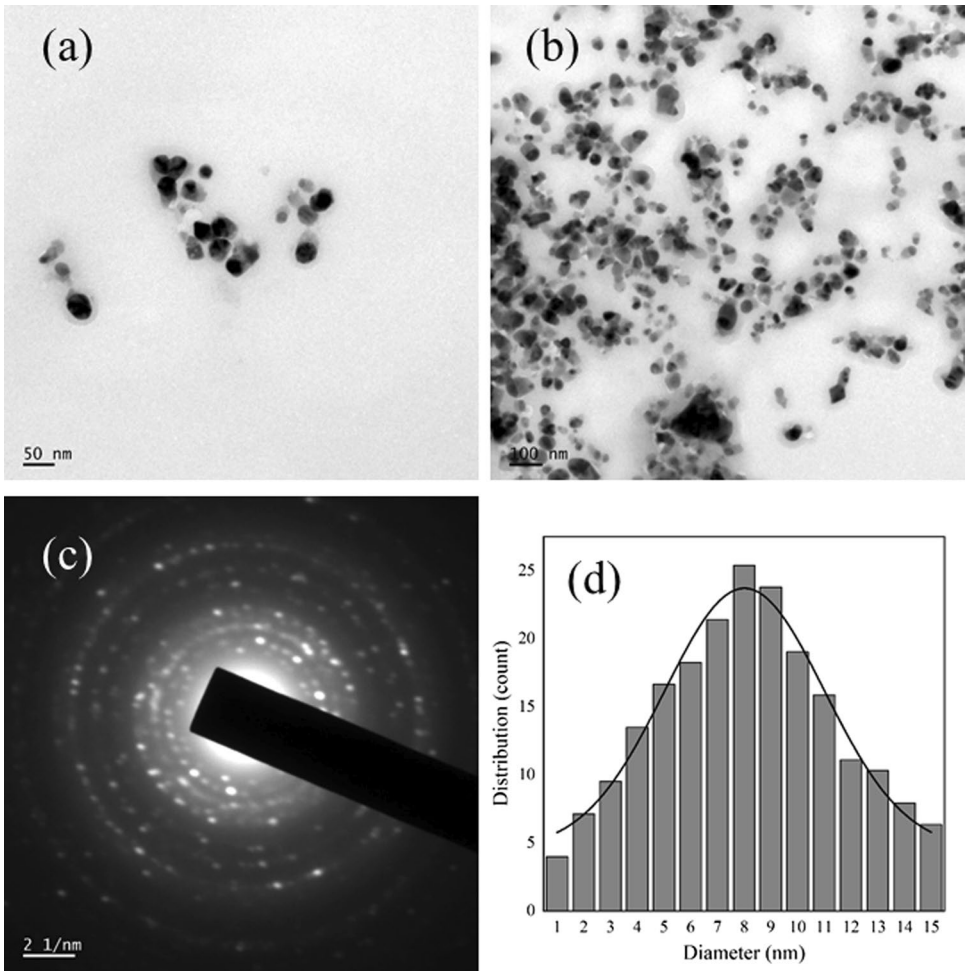

Fig. 5 TEM images **a**, **b** of silver nanoparticles from plant extract). **c** is the crystalline nature of the AgNPs, and **d** *image J* graph shows the average particles size

from plant extract worked as a capping agent. In this capping, organic material avoids the AgNPs aggregation, which gives more strength (Edison et al. 2016).

Fourier transforms infrared spectrometry of AgNPs

FTIR is used to explore the AgNPs chemical composition and the molecular background of the NPs. The functional groups of biosynthesized AgNPs from plant extract were identified by IR spectrum (scan range from 4000 to 400 cm^{-1}). Figure 6a shows the chemical bands of the biosynthesized AgNPs and plant extract. AgNPs showed extensive bands at 3325, 2122, 1739, 1634, 1365 and 1216 cm^{-1}. 3325 cm^{-1} assigned to the phenols and O–H bond, 2122 cm^{-1} assigned for C≡C bond of Terminal alkyne, 1739 cm^{-1} assigned to the C=O group asymmetrical and symmetrical stretching, 1634 cm^{-1} assigned to the primary amines for N–H bond, 1365 cm^{-1} assigned to ester C–O group and the extra band at 1216 cm^{-1} was assigned to the alkyl C–H stretching (Venil et al. 2016). FTIR study recommended that the hydroxyl groups of phenols and amide groups of proteins from plant extract form a layer to the NPs,

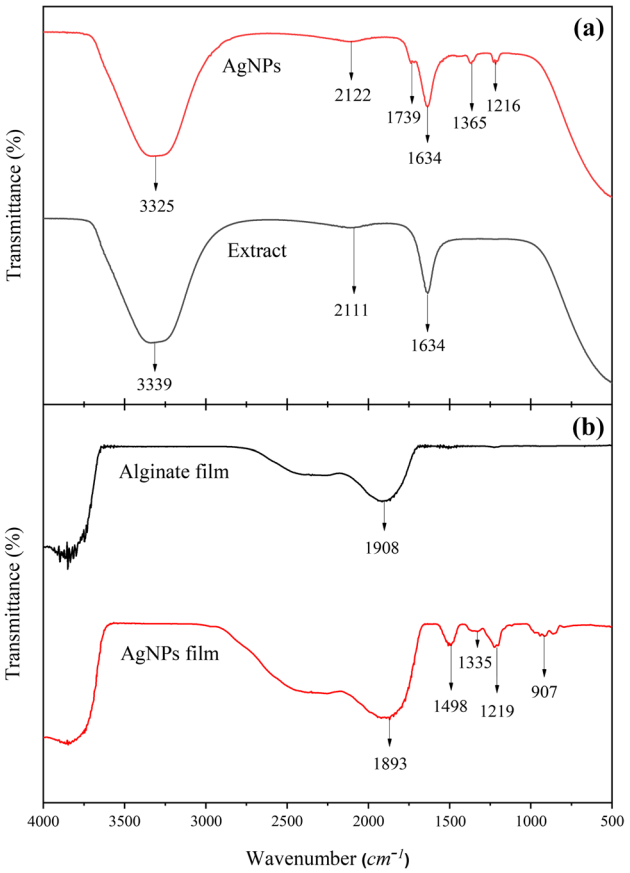

Fig. 6 FTIR results, **a** spectrums of bio-reduced AgNPs and plant extract, **b** peaks of AgNPs loaded film and neat sodium alginate film

act as a capping agent, give stability, and prevent agglomeration to the medium (Yugandhar and Savithramma 2016).

Scanning electron microscopy

Morphology of the biosynthesized AgNPs loaded SA films was analyzed using SEM analysis which gives the dispersion of NPs, and surface morphology. Figure 7 shows the AgNPs distribution on the AE film surface. AE composite film showed smooth surface morphology with the uniform distribution of AgNPs. TEM micrographs revealed the size of the AgNPs around 15 ± 10 nm, and it has a spherical shape. SA surface entirely coated with AgNPs, then again, the coverage of film surface by AgNPs on AE film significantly less as we can observe on SEM images Fig. 7. They also exhibited the existence of AgNPs with different shapes and some aggregation of the AgNPs on the surface.

Atomic force microscopy

Morphological images of AgNPs loaded alginate film (AE) (0.12 mm thickness) were characterized by AFM (contact mode) Fig. 7d. This analysis is mainly done to see the surface topography, distribution of NPs. From the 2D image, well-dispersed AgNPs were observed, and the image revealed that most of the NPs were in the range of 15–25 nm and appeared to be spherical which corresponds to the TEM and SEM results. The 3D image showed approximately the same NPs growth direction.

FT-IR analysis

FTIR is another essential technique to identify the interaction between SA and AgNPs, as shown in Fig. 6b. It was performed to estimate the specific adsorption of polymers, chemical bonds, and their dislocation toward wavelengths (lower or higher) caused by polymer functional groups interactions. The ALG spectrum at 1908 cm^{-1} corresponds to an asymmetric C=C bond. The presence of bands at 1893, 1498, 1335, 1219, and 907 cm^{-1} is due to the C–H stretching of aromatic bending, the strong N–O stretching, C–H stretching primary aromatic amine, the alkyl C–H stretching, and due to the alkene bending of C=C stretching, respectively (Venil et al. 2016). These results indicate that the proteins in secondary structures are not exaggerated as a consequence of response with AgNPs mixing. 1498 and 1335 cm^{-1} were due to the methylene scissoring vibration of the AE proteins (Mohammed Fayaz et al. 2009).

Contact angle measurements

Contact angle measurement was carried out to demonstrate the surface degree wettability of the SA and AE films.

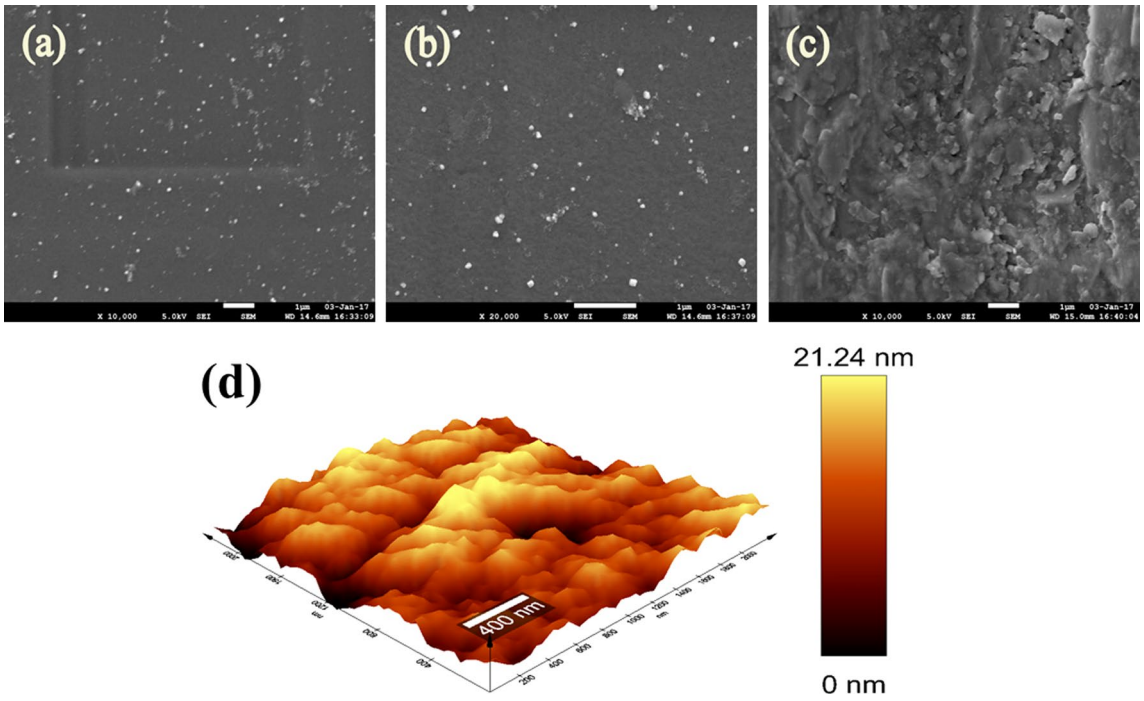

Fig. 7 Microscopic images, **a** FE-SEM images of AgNPs incorporated film at different magnifications with different scales and **c** cross-sectional magnification, **d** AFM images of AgNPs incorporated film (2%)

Figure 8 shows that the contact angle of SA film is 44° and AE film is 56°. A lower contact angle value indicates the hydrophilic nature of the SA film. At the same time, a higher contact angle value indicates less hydrophilicity. Compared to SA neat (ALG) film with AE film, AE has a higher contact angle due to the hydrophobic nature induced due to the interaction of free functional groups of SA with AgNPs. This decrease in hydrophilicity is desirable for various applications such as food packaging.

Mechanical analysis

Mechanical properties are an essential characterization technique for testing films. It could be used as an indicator of the film to maintain its strength, integrity and resist ecological stress throughout various applications. Mechanical properties of the SA and AE composite film's stress–strain curves are shown in Fig. 9a. This graph shows tensile strength, modulus, and elongation at break (values reported in Table 1). These are generally used to calculate the film samples' film flexibility, strength, and stiffness (Shankar et al. 2016). The ALG showed a tensile strength of 29.1 ± 1.4 MPa and an elongation at a break of 1.3 ± 0.06 (%). However, when compared to ALG film, the tensile strength of AE film was significantly increased to a value of (35 ± 1.75). The increase in tensile strength of AE film is due to the strong interaction between AgNPs and polymer matrix (Wang and Rhim 2015). This might be caused by the reduction in intra and inter–molecular chain interaction of sodium alginate due to the incorporation of AgNPs (Gudimalla et al. 2020). A tremendous increase in the modulus value from 497 ± 24.85 MPa to 833 ± 41.65 MPa shows the

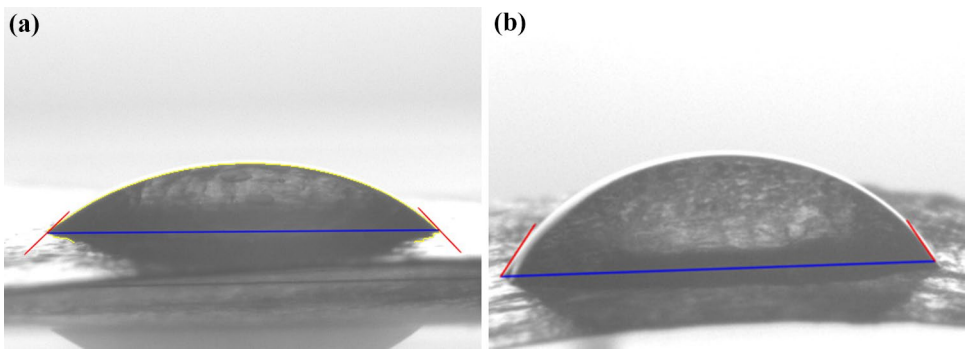

Fig. 8 Water contact angle of thin films **a** Neat sodium alginate film 44°, **b** AgNPs incorporated sodium alginate film 56°

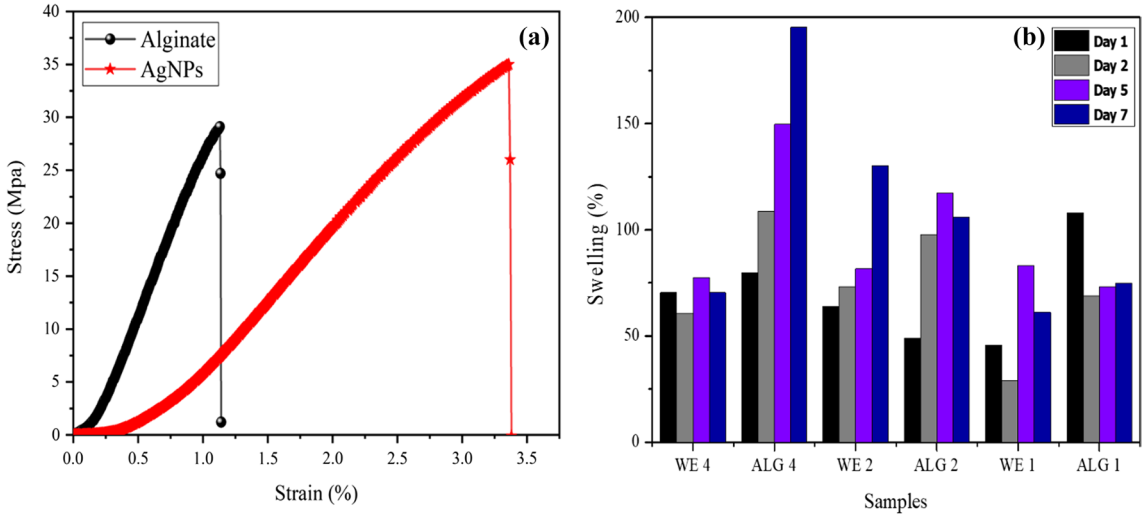

Fig. 9 (**a**) Tensile strength and elongation break of SA film (ALG) and AgNPs incorporated film (AE), **b** the swelling ratio of neat sodium alginate and AgNPs loaded films at different times intervals

Table 1 Tensile properties of AgNPs loaded film (AE) and neat sodium alginate film (ALG)

Samples	Elongation at break (%)	Modulus (MPa)	Tensile strength (MPa)
ALG	1.3 ± 0.06	497 ± 24.85	29.1 ± 1.45
AE	3 ± 0.15	833 ± 41.65	35 ± 1.75

Table 2 Water sensitivity tests of films such as Thickness, Moisture, Solubility, and Absorption. [AE-AgNPs loaded film, ALG-Neat sodium alginate film and (1, 2 and 4) different concentrations of the film]

Samples	Thickness (mm)	Moisture (%)	Solubility (%)	Absorption (%)
ALG4	0.232 ± 0.011	73.62 ± 3.68	14.48 ± 0.72	79.73 ± 3.9
AE4	0.176 ± 0.008	54.38 ± 2.71	12.65 ± 0.63	107.23 ± 5.36
ALG2	0.174 ± 0.008	46.50 ± 2.32	18.46 ± 0.92	48.92 ± 2.4
AE2	0.122 ± 0.006	50.55 ± 2.52	16.86 ± 0.84	149.62 ± 7.49
ALG1	0.194 ± 0.009	68.55 ± 3.42	14.72 ± 0.73	107.97 ± 5.3
AE1	0.184 ± 0.009	70.8 ± 3.54	32.65 ± 1.63	61.53 ± 3.07

excellent polymer-filler interaction. It is quite interesting to note that the presence of AgNPs imparts an increase in elongation at the break without compromising the tensile strength. This result shows the good strength and flexibility of the developed composites.

Films physical properties

Film thickness: SA and AE films thickness values are reported in Table 2. All neat SA (1, 2 and 4%) film thicknesses were found to be between 0.232 and 0.174 mm and AgNPs loaded films (1, 2 and 4%) between 0.184 and 0.122 mm; SA films were colorless, and the AE films showed the color. The values of different films are reported in Table 2. AE films showed less thickness when compared to ALG films. These results could be due to an integrated network between the chains of both polymers in the blends.

Moisture content ALG and AE film's moisture content values are reported in Table 2. The water content of the SA films was significantly decreased after the incorporation of AgNPs.

Water solubility The water solubility of films was used to measure the water resistance, and the values are reported in Table 2. The ALG2 film was showed the highest water solubility, around 18.4 ± 0.9. AE (4, 2 and 1%) films water solubility increased significantly while decreasing the concentration, AE4 film was given very less solubility 12.6 ± 0.6 at 37 °C. AE2 film solubility was around 16.8 ± 0.8; this value was increased when compared with the AE4 film. Finally, the AE1 film was showed the highest solubility at 32.6 ± 1.6; it shows very high solubility compared to AE2. These films were very thin, and even they had very low concentration. This reduction in the films' water solubility/moisture content is mainly due to the strong hydrogen bond formation between the AgNPs and the film matrix. The hydroxyl groups of extract capped AgNPs can form strong interactions through hydrogen bonds with the hydroxyl and carboxyl groups on alginate and improve the cohesiveness of the biopolymer matrix while decreasing water sensitivity.

Water absorption It was observed that the film samples showed high water absorption capacity, and the values are given in Table 2. AE films showed the highest swelling ratio compared to ALG films after incorporation of AgNPs water

uptake ratio was appreciably increased. Especially AE2 film showed 149.6 ± 7.4 water absorption ratios, at the same time, ALG2 film got lowest swelling 48.9 ± 2.4, it means after incorporation of AgNPs, the water absorption ratio was three times increased. The results were showed that the film capacity to absorb water is dependent on the medium value of pH. SA was protonated into unsolvable forms of alginic acid at lower pH values and will repel with the negative charged AgNPs, which influences the increase in swelling degree. AgNPs incorporation into the SA films contributes toward a slight increase in the film's water uptake for distilled water media, as shown in Table 2.

Swelling degree The composite films were submitted to a swelling degree with distilled water at 37 °C. It allowed evaluating the prepared composites water solubility and the ability of water uptake measurements. The film swelling ratios obtained and the significant period of time swelling values are reported in Fig. 9b. This established that the decreased swelling values, revealing the existence of dissolution, are attributable to the dissolution of cross-linked films gradually diffusing. ALG4 & 2% films showed slightly increasing day by day, and finally, it was shown highest swelling ratio. ALG1 film was shown day by day slightly changes; it was observed in Fig. 9b. AE 4, 2 and 1% films swelling ratio day by day decreased compared with ALG films observations shown in Fig. 9b. The water holding capacity of AE2 film increased profoundly compared with 4, 1%, and SA films.

Antimicrobial activity

It is well known that AgNPs, as well as silver ions, possess good antimicrobial activity. Antimicrobial activity was evaluated with *S. aureus* (Gram-positive) and *E. coli* (Gram-negative). This study was carried out by the well diffusion method, and the zone of inhibition (ZOI) was measured at different concentrations, as depicted in Fig. 10a. The diameters of the inhibition zone are reported in Table 3. The ZOI depends on the concentration of AgNPs. The inhibition zone diameter was (14–16 mm) and (16–18 mm), respectively. The high bactericidal activity of AgNPs is caused by their high surface area, which provides improved interaction with the bacteria (Zhang et al. 2016).

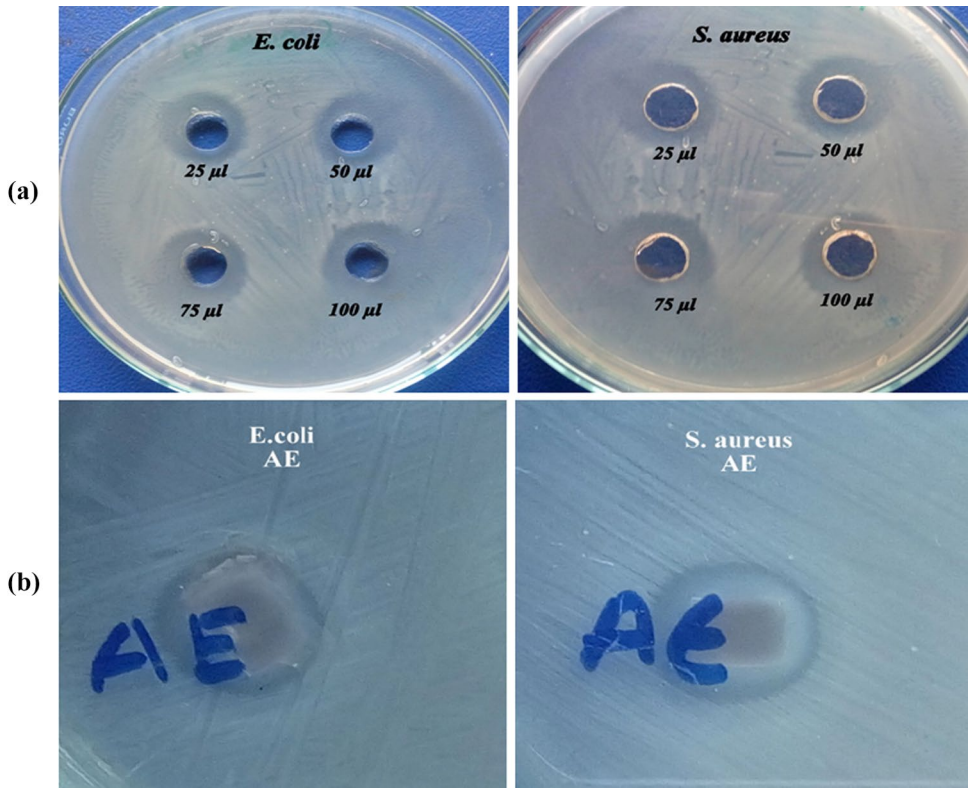

Fig. 10 (**a**) Zone inhibition of AgNPs against various microorganisms at different concentrations, **b** Antimicrobial activity of AgNPs loaded (AE) film

Table 3 AgNPs zone inhibition growth at different concentrations (mm)

AgNPs	*E. coli*				*S. aureus*			
	25 µL	50 µL	75 µL	100 µL	25 µL	50 µL	75 µL	100 µL
AE	14 ± 0.7	15 ± 0.7	15 ± 0.7	16 ± 0.8	16 ± 0.8	17 ± 0.8	17 ± 0.8	18 ± 0.9

Moreover, AgNPs act as reservoirs for the Ag^+ bactericidal agent. The NP activity occurs owing to the release of silver ions from the surface of AgNPs through oxidation. These ions act together with the enzymes and proteins, contributing to the disruption of cell development (Sohrabnezhad et al. 2015); smaller size NPs are further active and effective against microorganisms because of their superior capability to liberate silver ions (Gabriel et al. 2017). To this, TEM images revealed spherical shape and size 25 ± 10 nm. Thus, AgNPs prepared by natural medicinal plant extract might be an excellent antibacterial bio-resource with potential application in biomedical and related areas.

After that, we have evaluated the AgNPs incorporated film antimicrobial activity (Fig. 10b). The films were characterized by the disk diffusion method, and in this study, two types of microorganisms were used, such as *S. aureus* and *E. coli*. AE film zone of inhibition (ZOI) growth was observed. The results demonstrate that the AE film shows good antimicrobial activity against two pathogenic bacteria such as *S. aureus* and *E. coli*. Gram-negative bacteria showed 16 ± 0.8 mm of ZOI, while Gram-positive bacteria exhibited 14 ± 0.7 mm of ZOI.

This technique depends on the quantity of the ZOI due to the antimicrobial agent present in the film. AgNPs are well-known for being reactive and accordingly act together with the cell surface of the bacteria and finally killing them (Sharma et al. 2012). And it's capable of ZOI microbe development owing to its huge surface region, giving an excellent interaction among the microorganisms (Mokhena and Luyt 2017). The polymer nanocomposite film is estimated to stabilize for the long life of AgNPs. And, the AgNPs stabilization in a composite film depends on the polymer functional groups, which gives an electron to make interfacial linkage with the Ag^+ ions on the surface (Kamrupi et al. 2011). AgNPs composite film strength would also improve due to the communication of Ag^+ and functional groups. It is understood that the AgNPs antimicrobial activity depends not only on the shape and size of the particle but also on the AgNPs electrostatic charge. This charge plays a significant role (Shankar et al. 2016) in interaction among the pathogenic cell wall (negatively charged) and AgNPs (positive charged).

Conclusions

This study showed a facile, and green protocol for preparing AgNPs by the utilization of plant leaves which acted as both capping and reducing agents. The prepared NPs (size 15 ± 10 nm and spherical shape) were incorporated into a natural polymer which was further converted into composite films. After incorporating AgNPs, AE film tensile strength increased, and physical properties such as swelling, moisture content, and water uptake studies were improved. The prepared AE composite exhibited promising antimicrobial activity. The current green protocol of NP fabrication with subsequent incorporation into polymer films can potentially be used for wound dressings, food packing, and biomedical and biotechnology applications.

Acknowledgements This work was as a part of M.Sc. Project work of Mr. Apparao Gudimalla and self-funded research. The author AG great fully acknowledges and expresses thanks to International and Inter-University Center for Nanoscience and Nanotechnology, Mahatma Gandhi University, Kerala, India. He wants to express his thanks to Ms. Merina Luke for the valuable discussions and assistance in diffusion experiments during the course of the work.

Authors contribution AG and JJ conceived and designed the research work. AG conducted the all experiments, characterizations and wrote the manuscript. JVR edited and proof read the manuscript. JJ and ST contributed the laboratory facilities, reagents and analytical tools as well as supervised the research. All authors read and approved the manuscript.

Declarations

Ethical statement This article does not contain any studies with human participants or animals performed by any of the authors.

Conflict of interest The authors have no potential conflicts of interest to disclose.

References

Ahmed S, Ahmad M, Swami BL, Ikram S (2016) A review on plants extract mediated synthesis of silver nanoparticles for antimicrobial applications: a green expertise. J Adv Res 7:17–28. https://doi.org/10.1016/j.jare.2015.02.007

Ali G, Rihouey C, Larreta-Garde V, Le Cerf D, Picton L (2013) Molecular size characterization and kinetics studies on hydrolysis of pullulan by pullulanase in an entangled alginate medium. Biomacromol 14:2234–2241. https://doi.org/10.1021/bm400371r

Ali ZA, Yahya R, Sekaran SD, Puteh R (2016) Green Synthesis of Silver Nanoparticles Using Apple Extract and Its Antibacterial Properties. Adv Mater Sci Eng 2016:1–6. https://doi.org/10.1155/2016/4102196

Arunachalam KD, Annamalai SK, Shanmugasundaram H (2013) One-step green synthesis and characterization of leaf extract-mediated biocompatible silver and gold nanoparticles from Memecylon umbellatum. Int J Nanomed. https://doi.org/10.2147/ijn.s36670

Azlin-Hasim S, Cruz-Romero MC, Cummins E, Kerry JP, Morris MA (2016) The potential use of a layer-by-layer strategy to develop LDPE antimicrobial films coated with silver nanoparticles for packaging applications. J Colloid Interface Sci 461:239–248. https://doi.org/10.1016/j.jcis.2015.09.021

Barabadi H (2017) Nanobiotechnology: A promising scope of gold biotechnology. Cell Mol Biol 63:3. https://doi.org/10.14715/cmb/2017.63.12.2

Barabadi H, Honary S, Ebrahimi P, Alizadeh A, Naghibi F, Saravanan M (2019) Optimization of myco-synthesized silver nanoparticles by response surface methodology employing Box-Behnken design. Inorg Nano-Met Chem 49:33–43. https://doi.org/10.1080/24701556.2019.1583251

Daemi H, Barikani M, Sardon H (2017) Transition-metal-free synthesis of supramolecular ionic alginate-based polyurethanes. Carbohydr Polym 157:1949–1954. https://doi.org/10.1016/j.carbpol.2016.11.086

Duceppe N, Tabrizian M (2010) Advances in using chitosan-based nanoparticles forin vitroandin vivodrug and gene delivery. Expert Opin Drug Deliv 7:1191–1207. https://doi.org/10.1517/17425247.2010.514604

Edison TNJI, Lee YR, Sethuraman MG (2016) Green synthesis of silver nanoparticles using *Terminalia cuneata* and its catalytic action in reduction of direct yellow-12 dye. Spectrochim Acta Mol Biomol Spectrosc 161:122–129. https://doi.org/10.1016/j.saa.2016.02.044

Franci G, Falanga A, Galdiero S, Palomba L, Rai M, Morelli G, Galdiero M (2015) Silver nanoparticles as potential antibacterial agents. Molecules 20:8856–8874. https://doi.org/10.3390/molecules20058856

Gabriel JS, Gonzaga VAM, Poli AL, Schmitt CC (2017) Photochemical synthesis of silver nanoparticles on chitosans/montmorillonite nanocomposite films and antibacterial activity. Carbohydr Polym 171:202–210. https://doi.org/10.1016/j.carbpol.2017.05.021

Galus S, Lenart A (2013) Development and characterization of composite edible films based on sodium alginate and pectin. J Food Eng 115:459–465. https://doi.org/10.1016/j.jfoodeng.2012.03.006

Gudimalla A, Jose J, Varghese RJ, Thomas S (2020) Green synthesis of silver nanoparticles using *Nymphae odorata* extract incorporated films and antimicrobial activity. J Polym Environ 15:1–12. https://doi.org/10.1007/s10924-020-01959-6

Han J, Zhou Z, Yin R, Yang D, Nie J (2010) Alginate–chitosan/hydroxyapatite polyelectrolyte complex porous scaffolds: preparation and characterization. Int J Biol Macromol 46:199–205. https://doi.org/10.1016/j.ijbiomac.2009.11.004

Ionita M, Pandele MA, Iovu H (2013) Sodium alginate/graphene oxide composite films with enhanced thermal and mechanical properties. Carbohydr Polym 94:339–344. https://doi.org/10.1016/j.carbpol.2013.01.065

Iravani S (2011) Green synthesis of metal nanoparticles using plants. Green Chem 13:2638. https://doi.org/10.1039/c1gc15386b

Jemilugba OT, Sakho EHM, Parani S, Mavumengwana V, Oluwafemi OS (2019) Green synthesis of silver nanoparticles using *Combretum erythrophyllum* leaves and its antibacterial activities. Colloid Interface Sci Commun 31:100191. https://doi.org/10.1016/j.colcom.2019.100191

Kamrupi IR, Phukon P, Konwer BK, Dolui SK (2011) Synthesis of silver–polystyrene nanocomposite particles using water in supercritical carbon dioxide medium and its antimicrobial activity. J Supercrit Fluid 55:1089–1094. https://doi.org/10.1016/j.supflu.2010.09.027

Karakasyan C, Mathos J, Lack S, Davy J, Marquis M, Renard D (2015) Microfluidics-assisted generation of stimuli-responsive hydrogels based on alginates incorporated with thermo-responsive and amphiphilic polymers as novel biomaterials. Colloids Surf B 135:619–629. https://doi.org/10.1016/j.colsurfb.2015.08.028

Khatua A, Priyadarshini E, Rajamani P, Patel A, Kumar J, Naik A, Saravanan M, Barabadi H, Prasad A, Ghosh llora (2020) Phytosynthesis, characterization and fungicidal potential of emerging gold nanoparticles using *Pongamia pinnata* leave extract: a novel approach in nanoparticle synthesis. J Clust Sci 31:125–131. https://doi.org/10.1007/s10876-019-01624-6

Krishnaraj C, Jagan EG, Rajasekar S, Selvakumar P, Kalaichelvan PT, Mohan N (2010) Synthesis of silver nanoparticles using *Acalypha indica* leaf extracts and its antibacterial activity against water borne pathogens. Colloids Surf B 76:50–56. https://doi.org/10.1016/j.colsurfb.2009.10.008

Kulkarni RV, Boppana R, Krishna Mohan G, Mutalik S, Kalyane NV (2012) pH-responsive interpenetrating network hydrogel beads of poly(acrylamide)-g-carrageenan and sodium alginate for intestinal targeted drug delivery: synthesis, in vitro and in vivo evaluation. J Colloid Interface Sci 367:509–517. https://doi.org/10.1016/j.jcis.2011.10.025

Ma S, Chen Z, Qiao F, Sun Y, Yang X, Deng X, Cen L, Cai Q, Wu M, Zhang X (2014) Guided bone regeneration with tripolyphosphate cross-linked asymmetric chitosan membrane. J Dent 42:1603–1612. https://doi.org/10.1016/j.jdent.2014.08.015

Matricardi P, Di Meo C, Coviello T, Hennink WE, Alhaique F (2013) Interpenetrating polymer Networks polysaccharide hydrogels for drug delivery and tissue engineering. Adv Drug Deliv Rev 65:1172–1187. https://doi.org/10.1016/j.addr.2013.04.002

Mohammed Fayaz A, Balaji K, Girilal M, Kalaichelvan PT, Venkatesan R (2009) Mycobased synthesis of silver nanoparticles and their incorporation into sodium alginate films for vegetable and fruit preservation. J Agric Food Chem 57:6246–6252. https://doi.org/10.1021/jf900337h

Mokhena TC, Luyt AS (2017) Electrospun alginate nanofibres impregnated with silver nanoparticles: Preparation, morphology and antibacterial properties. Carbohydr Polym 165:304–312. https://doi.org/10.1016/j.carbpol.2017.02.068

Nabikhan A, Kandasamy K, Raj A, Alikunhi NM (2010) Synthesis of antimicrobial silver nanoparticles by callus and leaf extracts from saltmarsh plant, *Sesuvium portulacastrum* L. Colloids Sur B 79:488–493. https://doi.org/10.1016/j.colsurfb.2010.05.018

Olivas GI, Barbosa-Cánovas GV (2008) Alginate–calcium films: Water vapor permeability and mechanical properties as affected by plasticizer and relative humidity. LWT 41:359–366. https://doi.org/10.1016/j.lwt.2007.02.015

Orsuwan A, Shankar S, Wang L-F, Sothornvit R, Rhim J-W (2016) Preparation of antimicrobial agar/banana powder blend films reinforced with silver nanoparticles. Food Hydrocolloids 60:476–485. https://doi.org/10.1016/j.foodhyd.2016.04.017

Pauksch L, Hartmann S, Rohnke M, Szalay G, Alt V, Schnettler R, Lips KS (2014) Biocompatibility of silver nanoparticles and silver ions in primary human mesenchymal stem cells and osteoblasts. Acta Biomater 10:439–449. https://doi.org/10.1016/j.actbio.2013.09.037

Puppi D, Zhang X, Yang L, Chiellini F, Sun X, Chiellini E (2014) Nano/microfibrous polymeric constructs loaded with bioactive agents and designed for tissue engineering applications: a review. J Biomed Mater Res B 102:1562–1579. https://doi.org/10.1002/jbm.b.33144

Rani P, Mishra S, Sen G (2013) Microwave based synthesis of polymethyl methacrylate grafted sodium alginate: its application as flocculant. Carbohydr Polym 91:686–692. https://doi.org/10.1016/j.carbpol.2012.08.023

Roldán MV, de Oña P, Castro Y, Durán A, Faccendini P, Lagier C, Grau R, Pellegri NS (2014) Photocatalytic and biocidal activities of novel coating systems of mesoporous and dense TiO2-anatase containing silver nanoparticles. Mater Sci Eng C 43:630–640. https://doi.org/10.1016/j.msec.2014.07.053

Sanpui P, Chattopadhyay A, Ghosh SS (2011) Induction of apoptosis in cancer cells at low silver nanoparticle concentrations using chitosan nanocarrier. ACS Appl Mater Interfaces 3:218–228. https://doi.org/10.1021/am100840c

Shankar S, Wang L-F, Rhim J-W (2016) Preparations and characterization of alginate/silver composite films: effect of types of silver particles. Carbohydr Polym 146:208–216. https://doi.org/10.1016/j.carbpol.2016.03.026

Sharma S, Sanpui P, Chattopadhyay A, Ghosh SS (2012) Fabrication of antibacterial silver nanoparticle—sodium alginate–chitosan composite films. RSC Adv 2:5837. https://doi.org/10.1039/c2ra00006g

Shi J, Kantoff PW, Wooster R, Farokhzad OC (2017) Cancer nanomedicine: progress, challenges and opportunities. Nat Rev Cancer 17:20–37. https://doi.org/10.1038/nrc.2016.108

Sikareepaisan P, Ruktanonchai U, Supaphol P (2011) Preparation and characterization of asiaticoside-loaded alginate films and their potential for use as effectual wound dressings. Carbohydr Polym 83:1457–1469. https://doi.org/10.1016/j.carbpol.2010.09.048

Sohrabnezhad Sh, Pourahmad A, Mehdipour Moghaddam MJ, Sadeghi A (2015) Study of antibacterial activity of Ag and Ag2CO3 nanoparticles stabilized over montmorillonite. Spectrochim Acta Mol Biomol Spectrosc 136:1728–1733. https://doi.org/10.1016/j.saa.2014.10.074

Tetgure SR, Borse AU, Sankapal BR, Garole VJ, Garole DJ (2015) Green biochemistry approach for synthesis of silver and gold nanoparticles using *Ficus racemosa* latex and their pH-dependent binding study with different amino acids using UV/Vis absorption spectroscopy. Amino Acids 47:757–765. https://doi.org/10.1007/s00726-014-1906-9

Venil CK, Sathishkumar P, Malathi M, Usha R, Jayakumar R, Yusoff ARM, Ahmad WA (2016) Synthesis of flexirubin-mediated silver nanoparticles using *Chryseobacterium artocarpi* CECT 8497 and investigation of its anticancer activity. Mater Sci Eng C 59:228–234. https://doi.org/10.1016/j.msec.2015.10.019

Wang L-F, Rhim J-W (2015) Preparation and application of agar/alginate/collagen ternary blend functional food packaging films. Int J Biol Macromol 80:460–468. https://doi.org/10.1016/j.ijbiomac.2015.07.007

Yugandhar P, Savithramma N (2016) Biosynthesis, characterization and antimicrobial studies of green synthesized silver nanoparticles from fruit extract of *Syzygium alternifolium* (Wt.) Walp. an endemic, endangered medicinal tree taxon. Appl Nanosci 6:223–233. https://doi.org/10.1007/s13204-015-0428-4

Zain NM, Stapley AGF, Shama G (2014) Green synthesis of silver and copper nanoparticles using ascorbic acid and chitosan for antimicrobial applications. Carbohydr Polym 112:195–202. https://doi.org/10.1016/j.carbpol.2014.05.081

Zhang X, Su Z (2012) Polyelectrolyte-multilayer-supported Au@Ag core-shell nanoparticles with high catalytic activity. Adv Mater 24:4574–4577. https://doi.org/10.1002/adma.201201712

Zhang S, Tang Y, Vlahovic B (2016) A review on preparation and applications of silver-containing nanofibers. Nanoscale Res Lett 11:1–8. https://doi.org/10.1186/s11671-016-1286-z